RSC Advances

ROYAL SOCIETY OF CHEMISTRY

www.rsc.org/advances

Journal Name ARTICLE

Cellulose nanofibrils: a rapid adsorbent for the removal of methylene blue

Chi Hoong Chan, Chin Hua Chia*, Sarani Zakaria, Mohd Shaiful Sajab and Siew Xian Chin

Cellulose nanofibrils (CNF) were prepared from kenaf core (KC) using acidified-chlorite bleaching method and followed by disintegration using high speed blender. The effects of disintegration time and acid treatment on the defibrillation of holocellulose were studied. Hemicellulose was found to facilitate defibrillation, as CNF without any acid treatment was fully defibrillated after 30 min. The adsorption kinetics of CNF toward cationic dye cannot be accurately determined due to its quick adsorption performance, in which the equilibrium is achieved immediately after 1 min of contact time. The effects of acid treatment on holocellulose, pH, adsorbent dosage, temperature and dye concentration were studied and optimized. Adsorption data were fitted to both Langmuir and Freundlich models where Langmuir model was found to be the better model to describe the adsorption process. Maximum adsorption capacity was found to be 122.2 mg/g at pH 9, 20 °C for the non-acid treated CNF. The CNF can be regenerated by desorption at low pH where, as much as 70 % of dye adsorbed can be desorbed after 6 cycles of adsorption-desorption cycle.

Cite this: DOI: 10.1039/x0xx00000x

Received 00th January 2012,

Accepted 00th January 2012

DOI: 10.1039/x0xx00000x

www.rsc.org/

Journal Name RSCPublishing

ARTICLE

Introduction

The demand for clean water is ever increasing, fuelled by rapid urbanization and expanding industrial activities. This demand cannot be serviced by fresh water sources alone and must be met by utilizing wastewater treatment techniques. However, the type of treatment depends heavily on the kinds of contaminants and pollutants which exist within the wastewater source. For example, industrial contaminants can include heavy metals [1], volatile organic compounds [2], dyes [3], etc which can cause various type of health ailments if exposed to end users. In the case of dye, it is estimated that annual world production of dyes to be 10 Mt [4], where 10 - 15 % of dyes used are lost during dyeing process. This is just one of the many examples of organic effluent discharged into the environment. Although industrial treatments for cationic contaminants do exist, it is limited by the availability of chemicals used for treatment and requires the usage of specialized adsorbent. Therefore, alternative types of treatment methods which are reliable, effective and cost efficient needs to be developed to combat this threat on a larger scale.

A promising material which could be turned into adsorbent is cellulose nanofibrils (CNF). It has already been demonstrated that cellulose nanocrystals can be a good adsorbent for cationic dye [5, 6], while CNF aerogel has a low adsorption capacity [7]. Cellulose nanofibrils, (CNF) are cellulose microfibrils extracted from cellulose pulp through mechanical means. The terms, nanofibrillated cellulose (NFC), cellulose nanofibrils (CNF), cellulose microfibrils (MCF), microfibrillated cellulose (MFC) and sometimes nanofibers are used interchangeably to refer to defibrillated wood pulp by physical means with chemical, enzymatic or physical pre-treatments [8, 9]. In this paper, the term CNF is used.

The process typically begins using readily available bleached kraft pulp or sulfite pulp) [10-12]. The pulp can then undergo one of the various methods to defibrillate cellulose, namely, high-pressure homogenization [13], grinding [14], steam explosion [15], etc. These methods are very energy extensive [16], but the energy cost can be mitigated by pre-treatment. Pre-treatment usually aims to limit the hydrogen bonding, adding a repulsive charge on the surface of CNF and decreasing the degree of polymerization [17]. A suitable pre-treatment is carboxylation, which involves oxidation of macrofibrils which induces carboxylation on the cellulose surface so as to facillitates the second disintegration step. Carboxylation can be performed using 2,2,6,6-tetramethylpiperidine-1-oxyl radical (TEMPO) mediated oxidation [18], enzymatic [19] and acidified chlorite [20].

Another factor in the processing of CNF is lignin content. Lignin and hemicellulose form the matrix in natural fibers while cellulose reinforces it. Therefore, to extract CNF, a precursor with a low lignin content is preferable. Acidified chlorite bleaching can be used for lignin removal and carboxylating its surface although this process was originally used to determined holocellulose content [21]. This delignification method is also less harsh to cellulose while highly selective of lignin [22].

CNF has a wide and potential applications, such as, reinforcement in composites [23, 24], thickening agent in food and paint [25], in electronic devices [26], scaffold for tissue growth [27], etc. While, cellulose nanocrystals (CNC) had been demonstrated to be a good adsorbent for cationic dye [6, 5], CNF had yet to be demonstrated.

In this paper, we demonstrated that CNF with varying hemicellulose can be prepared easily using acid hydrolysis treatment. We also demonstrated that CNF is a rapid adsorbent for cationic dye without any further chemical modification. To the best of our knowledge, this study is the first (if not the first) demonstration of CNF derived from holocellulose used to remove toxic dye.

Experimental

Materials

Kenaf core (KC) powder (60-80 mesh) was obtained from Malaysian Agricultural Research and Development Institute (MARDI). Sigmacell Cellulose Type 20 (Sigma-Aldrich), sodium chlorite, 80 % (Acros Organics), glacial acetic acid, 95 % (R&M Chemicals), hydrochloric acid, 32 % (JT Baker), sodium hydroxide, 99 % (Merck), sulfuric acid, 98% (HmbG Chemicals), calcium carbonate, AR Grade (Bendosen) and methylene blue trihydrate (Mallinckrodt, ≥99%) were used as received without further purification. Water used was purified by arium Pro ultrapure water system with a conductivity of 18.2 MΩ·cm (Sartorius Stedim). All fibers used before and after treatment or experiment were never dried unless stated.

ATR-FTIR

Attenuated total reflectance (ATR) FTIR (Perkin-Elmer Spectrum 400) was used to analyze all samples. KC, KC holocellulose and cellulose nanofibrils of different hydrolysis treatment times were freeze-dried prior to the scanning in a resolution of 1 cm^{-1} and range of 4000-650 cm^{-1}.

Delignification and Defibrillation

The KC powder was rinsed a few times with distilled water to remove impurities present during processing. Delignification was performed using acid-chlorite bleaching [21], six times for a total of 1.875 g/g of sodium chlorite and 1.25 g/g of acetic acid. *In-situ* acid hydrolysis treatments using 2.5 M HCl at 45°C at various times, 10, 30 and 90 min were conducted to obtain KC holocellulose of varying hemicellulose contents. After each treatment, the sample was washed with distilled water and rinsed with ultrapure water until neutrality before nanofibrillation process.

To observe the effect of hemicellulose on the nanofibrillation process, KC holocellulose of varying hemicellulose contents were agitated in a high speed blender (Vitamix, Vita-Prep 3) at 0.7 wt.% in 0.1 mM of NaCl as counterion for 30 min.

Compositional Analysis

The composition of all samples was analyzed according to laboratory procedures of National Renewable Energy Laboratory (NREL) [28]. KC, KC holocellulose and CNF of different treatment were freeze-dried prior to the composition analysis. High-performance liquid chromatography (HPLC) system (Agilent 1260) equipped with Agilent, Hi-Plex H and Hi-Plex Pb columns. Refractive index (RI) and UV detectors were used to measure the concentration of glucose, xylose, galactose, mannose, arabinose, acetic acid, 5-HMF and furfural of the hydrolysis liquor. The temperature of the column and detector was set at 60 and 55 °C, respectively, while a mobile phase 5 mmol H_2SO_4 was used at a flow rate of 0.6 mL/min. All analyses were carried out in duplicate and the mean value was used.

TEM

Micrographs of transmission electron microscopy (TEM, CM 12 Phillips) for the KC holocellulose and CNF of different agitation time and treatment were captured. A drop of diluted suspension of the sample in ethanol (*ca.* 0.01 wt.%) was dropped onto a copper grid and stained with uranyl acetate, 3 wt.%. At least 160 measurements of CNF diameters were made for each sample.

Adsorption

Preparation of dye solutions

Methylene blue (MB) trihydrate solutions were prepared and diluted accordingly to the required initial concentration. The concentration of MB in working solutions was measured using a UV-Vis spectrophotometer (Jenway 7315 Spectrophotometer) at a λ_{max} of 665 nm. A standard calibration curve, fitted by the Beer-Lambert's law, was prepared from the MB solutions with different concentrations that yielded absorbance ranging from 0.1 to 1.

Adsorption Kinetic Studies

Adsorption kinetics experiments of MB on CNF, KC and Sigmacell at room temperature were carried out. Briefly, 0.1 g of adsorbent was added into a flask containing 100 mL of dye solution (100 mg/L). Aliquots of solution (~ 0.1 mL) were withdrawn at various time intervals and filtered immediately using nylon-membrane syringe filter (Agilent, 0.2 μm) and its concentration (MB) was determined using the spectrophotometer. The amount of dye adsorbed per unit mass of adsorbent at time *t,* q_t (mg/g) was calculated using equation below.

$$q_t = \frac{(C_0 - C_t)V}{m} \quad (1)$$

where C_0 and C_t are the initial concentration and concentration of dye at time, *t*, (mg/L), while m and V is the mass of adsorbent (g) and volume of dye solution (L).

Adsorption Studies

A similar procedure as described above was employed to investigate the adsorption performance towards MB of different initial pHs, ranging from pH 3 to 9. The initial pH was pre-adjusted using 0.01 M of HCl or 0.01 M of NaOH and stirred at 250 rpm for 2 min. To evaluate the adsorption isotherms, adsorption experiments using dye concentrations (50 - 300 mg/L) were carried out at a different fixed temperature (20, 40 and 60 °C). The concentration of dye in the supernatant solution (C_e) was determined using the spectrophotometer. The amount of dye adsorbed per unit mass of fibres (q_e) was calculated using equation below.

$$\text{Dye adsorbed}\,(\%) = \frac{(C_0 - C_e)}{C_0} \times 100\,\% \quad (2)$$

$$q_e = \frac{(C_0 - C_e)V}{m} \quad (3)$$

Desorption and Regeneration

CNF samples used for the adsorption of 100 mg/L of MB solutions were washed using deionized water, centrifuged and remove the remaining of MB. About 0.1 g of the CNF were treated with 100 mL of HCl (0.1 M) and the amount of dye desorbed was determined spectrophotometrically and calculated using equation below

$$\text{Dye desorbed}\,(\%) = \frac{\text{Conc. desorbed (mg/L)}}{\text{Conc. adsorbed (mg/L)}} \times 100\,\% \quad (4)$$

The regenerated CNF were then repeated for six consecutive adsorption-desorption processes.

Results and Discussion

Compositional Analysis

The major components of lignocellulosic materials are composed of carbohydrates and lignin. The components in KC from cellulose consist of β (1 → 4)-D-glucopyranose and from hemicellulose β (1 → 4)-D-xylopyranose and 4-O-methyl-glucuronic acid [29]. In order to investigate the effects of hemicellulose on the degree of fibrillation of holocellulose, it was treated in acid and its composition was determined analytically. The KC holocellulose samples treated with acid for 10, 30, 90 and 180 minutes are designated as AH10, AH30, AH90 and AH180 respectively.

Table 1 Components in CNF and its components after acid treatment at various time

Sample (mass fraction, %)	Kenaf Core	CNF	AH10	AH30	AH90	AH180
Total Xylan[a]	18.49 ± 0.07	23.29 ± 0.20	23.14 ± 0.14	22.90 ± 0.14	22.35 ± 0.13	21.31 ± 0.13
Total Acetyl	8.39 ± 0.34	7.25 ± 0.12	6.38 ± 0.11	5.35 ± 0.08	4.03 ± 0.06	3.29 ± 0.04
Total Cellulose	37.75 ± 0.79	55.77 ± 0.80	56.53 ± 0.79	57.56 ± 0.82	60.19 ± 0.75	65.69 ± 0.96
Total Lignin (soluble)[b]	4.97 ± 0.11	8.22 ± 0.39	7.83 ± 0.22	7.75 ± 0.17	7.40 ± 0.23	6.98 ± 0.19
Total Lignin (insoluble)	23.62 ± 0.54	0.64 ± 0.19	0.60 ± 0.15	1.11 ± 0.18	0.83 ± 0.12	0.98 ± 0.15

[a] Arabinose cannot be detected while small amount of galactose and mannose are detected. The amount is too low to be quantitatively accurate, therefore, only xylan content is reported. [b] hydroxymethyl furfural and furfural are detected by HPLC, although the amount is low, it may inflate the value of Total Lignin (soluble). The concentration of hydroxymethyl furfural and furfural are compiled in Table S1.

Initially, the KC sample consists of total cellulose, 37.75 ± 0.79 and total hemicellulose (xylan and acetyl) of 26.88 ± 0.42. The yield of holocellulose from the kenaf core is *ca.* 55 % due to fiber lost during washing and hydrolysis of cellulose and hemicellulose during delignification process. After delignification, the mass fractions of cellulose and hemicellulose increased due to removal of lignin. Overall, delignification removed *ca.* 98 % of acid-insoluble lignin but only removed *ca.* 9 % of acid-soluble lignin while retaining hemicellulose. Some residual lignin remained bonded to xylan chain after delignification process because it is not acid-labile [30] and present along CNF. By treating holocellulose in acid at various times we managed to obtain samples with different hemicellulose contents. Holocellulose treated with acid at low temperature is mild enough to preferentially hydrolyse hemicellulose while leaving cellulose structure intact [31, 32]. Acid treatment hydrolyzes β (1 → 4)-D-xylopyranose and O-acetylated xylopyranose to xylose and acetic acid respectively. After acidic treatment with increasing time, total xylan decrement is low, however, acetyl content decreases significantly. By plotting the reciprocal of residual hemicellulose content (total xylan and total acetyl) versus time, a second order kinetics for removal of hemicellulose can be observed (Fig. S1). However, we are unable to replicate the quick removal of hemicellulose from holocellulose as reported previously by Foston *et al.* [31]. We also analyzed the liquid in CNF after agitation in high speed blender using HPLC and found that no sugar is present.

TEM

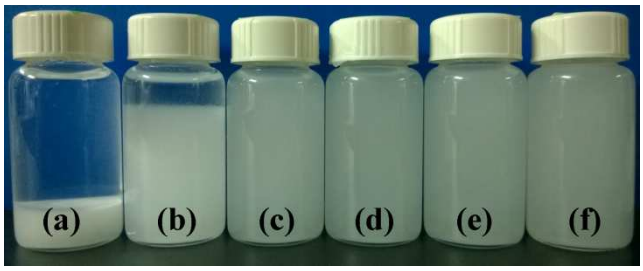

Fig. 1 Holocellulose of different agitation time, (a) 0 min, (b) 1 min, (c) 5 min, (d) 10 min, (e) 20 min and (f) 30 min.

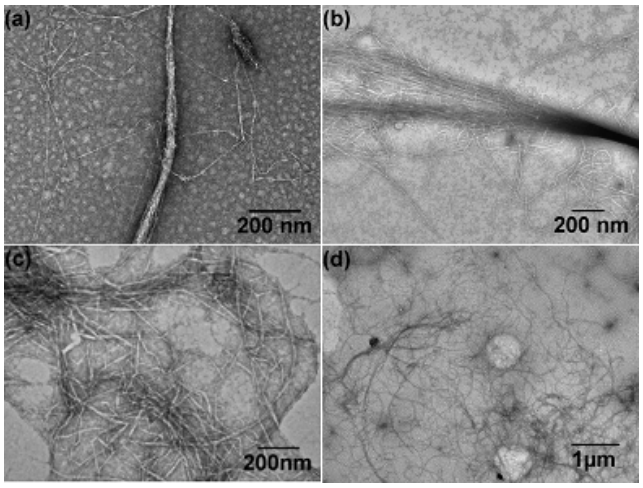

Fig. 2 TEM images of holocellulose with different agitation times, (a) 0 min, (b) 10 min, (c) 30 min and (d) 50 min.

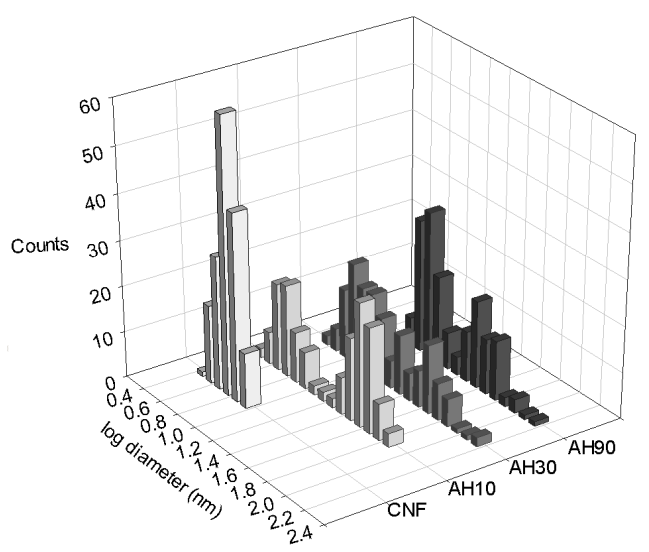

Fig. 3 Distribution of CNF diameters with varying acid treatment time.

The stability of the samples was observed by storing them at 4 °C for 1 month. Only 5 min of agitation is required to produce a stable defibrillated holocellulose suspension from visual observation as shown in Fig. 1. To find the optimum time of defibrillation for holocellulose, sampling was performed at 0, 10, 30 and 50 min of defibrillation and the sample was observed under TEM.

In the non-agitated holocellulose, Fig. 2 (a), macrofibrils can be clearly seen. Even without agitation, some cellulose nanofibrils can be observed protruding out from macrofibrils, however, no individualized microfibrils can be observed. After 10 min of agitation, macrofibrils are now partially defibrillated into aggregated CNF. Aggregated CNF and individual microfibrils can be seen diverging from macrofibril as seen in Fig. 2 (b). The diameter of macrofibrils in Fig. 2 (a) and (b) was found to be between 45 - 93 nm, while for Fig. 2 (b), the diameter of microfibrils was found to be between 3.2 and 12.9 nm, with an average of 6.5 nm. After 30 min of agitation (Fig. 2 (c)), no macrofibrils can be observed. Aggregated and individual microfibrils formed a web-like structure with some bent microfibrils. The CNF observed were either aggregated or individualized where the diameter observed was found to be between 3.0 - 9.6 nm with an average of 5.5 nm. After 50 min of agitation (Fig. 2 (d)), breakage can be observed and CNF are comparatively shorter in length than the CNF of 30 min of agitation. Looping, bending and twisting of microfibrils can also be observed after 50 min of agitation. Diameters were found to be between 3.3 - 8.5 nm, with an average of 5.7 nm.

From the TEM observations, by agitating holocellulose in a high speed household blender, CNF were successfully produced from KC. Using blender as a nanofibrillation unit had also been demonstrated previously [18, 33-35]. The optimum time of defibrillation is 30 min where no macrofibrils was observed and the CNF were less damaged as compared to 50 min of defibrillation. This is in agreement with previous study done by Uetani *et al.* [33].

To investigate the effects of acid treatment on the degree of defibrillation, acid treated holocellulose were defibrillated for 30 min in the high speed blender and observed under TEM. To better visualize the changes in diameters of the CNF, the recorded diameters of the CNF are plotted in logarithmic diameter (nm). By increasing the acid treatment time, the degree of defibrillation decreases after 30 min of agitation (Fig. S2). The incomplete defibrillation of the acid treated holocellulose may be due to the reduction of hemicellulose content [20, 34]. No macrofibrils can be observed for non-acid treated CNF while macrofibrils or partially defibrillated macrofibrils can be observed for all acid treated samples as evidenced by the emergence of double peaks of diameter distribution as shown in Fig. 3. A double peak of diameter distribution is observed are due to individualized and partially defibrillated macrofibrils. An indirect evaluation for the degree of defibrillation using UV-Vis spectrophotometer confirms the incomplete defibrillation of acid treated holocellulose as evidenced by the decrease in light transmittance (Fig. S3).

Diameter of CNF increases with increasing acid treatment time. For example, CNF diameters of > 10 nm increases from 0 %, 58.1 %, 61.3 % and 78.1 % for CNF, AH10, AH30 and AH90 respectively.

ATR-FTIR

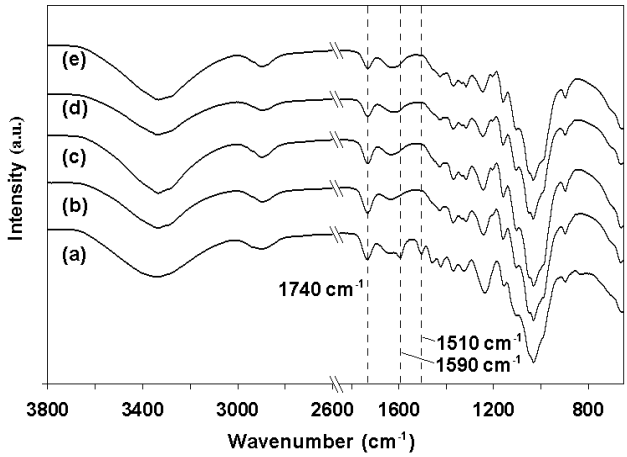

Fig. 4 FTIR-ATR spectra for (a) KC, (b) CNF, (c) AH10, (d) AH30 and (e) AH90

ATR-FTIR was used to determine the delignification efficiency and functional groups present on the surface of the samples. Fig. 4 shows the IR spectra for KC, CNF and acid treated CNF. All samples showed the characteristics peaks for cellulose, i.e., 3340 cm^{-1}, 2901 cm^{-1}, 1640 cm^{-1} and 1163 cm^{-1} are responsible for the O-H stretching, due to intermolecular hydrogen bonding [36], aliphatic alkyls stretching [36], adsorbed water and ether linkages of pyranose ring [37] respectively. Characteristic peak of hemicellulose, 1731 cm^{-1}, due to carbonyl (ester linkage), is retained after the delignification process. However, the carbonyls can be attributed to carbonyls in lignin [38] and carboxylation during the delignification process [35]. After delignification, characteristics peaks for lignin, 1590 cm^{-1} and 1510 cm^{-1} [37], which belongs to aromatic symmetric

and aromatic asymmetric stretching, cannot be observed. However, from the compositional analysis, > 8 % of lignin still remains after the delignification. No peaks can be observed from 2800 - 1800 cm^{-1} region.

Rapid Adsorption of CNF

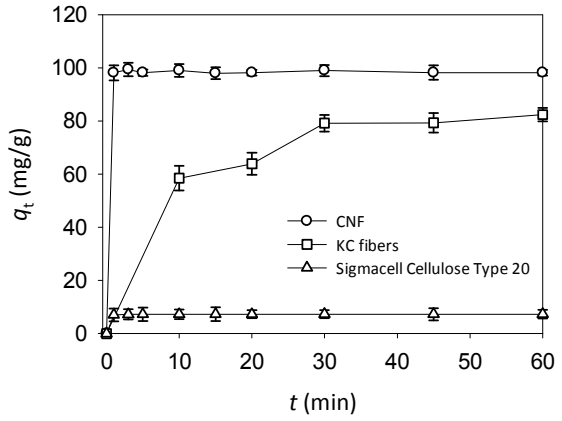

Fig. 5 Rapid adsorption of CNF compare to KC towards MB (Temperature: 20 °C; adsorbate dose: 100 mg/L)

Adsorption equilibrium for CNF in 100 mg/ml of MB was achieved after 1 min of contact time while for KC and Sigmacell are both 30 min. The adsorption kinetics for CNF cannot be accurately determined due to its rapid adsorption performance. This can be explained by the morphology and a lack of well-defined structure in the CNF. CNF is a one-dimensional (1D) material consisting of a long chain (aspect ratio, > 100), non-homogeneous [39] and entangled network of cellulose [40]. As such, CNF suspension in water contains no pores as opposed to KC and Sigmacell. In conventional theory of adsorption for activated carbon for example, there are two adsorption mechanisms, firstly, adsorbate must first be in contact with adsorbent (mass transfer of adsorbate) then the filling of pores due to capillary forces (diffusion of adsorbate through pores). The rate determining step is the diffusion of adsorbate (slow rate) which is a function of time, due to capillary action which translates to adsorption kinetics. However, there are no pores in CNF suspension, hence; the kinetics of adsorption is solely dependent on the mass transfer.

Adsorption Studies

Effect of Initial pH

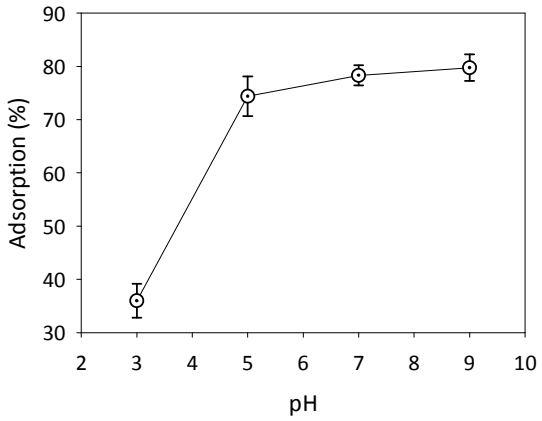

Fig. 6 Effect of pH on adsorption capacity of CNF towards MB (Temperature: 20 °C; adsorbate dose: 100 mg/L)

The effect of pH on the adsorption capacity of the CNF towards MB is shown in Fig. 6. The pH of medium affects the surface charge of the adsorbents, for cationic dye adsorbents, the surface charge decreases with decrement of pH. This translates to adsorption performance and plausibility of regeneration i.e., through desorption at low pH. The CNF adsorbent works best at higher pH while adsorbing as low as 35 % of total dye at pH 3. Similar to other studies using KC and treated KC [41] and cellulose nanocrystals (CNC) [6], adsorption performance at low pH is lowered due to higher competition between dye molecules and H^+ ions to form electrostatic attraction [42, 43]. This also suggests that dye can be desorbed at low pH for regeneration studies.

Adsorption Isotherms

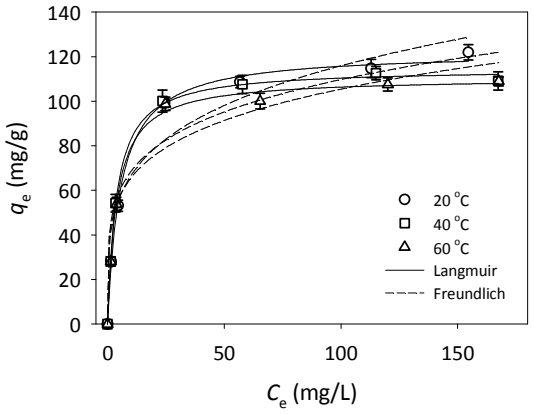

Fig. 7 Non-linearized isotherm plots of Langmuir and Freundlich for the adsorption of MB on CNF at various temperatures.

Langmuir and Freundlich isotherms are applied to describe the adsorption process by plotting q_e vs. C_e in Fig. 7. Both isotherms have been widely used for adsorption experiment data fitting. Langmuir isotherm assumes monolayer coverage of

adsorbate over a homogeneous adsorbent surface where each molecule adsorbed onto its surface requires equal adsorption activation energy. Additionally, for Langmuir isotherm, no adsorbate migration occurs after adsorption. Freundlich isotherm describes reversible adsorption and is not restricted to the formation of monolayer [44]. The Langmuir isotherm equation is shown as follow:

$$q_e = \frac{Q_0 b C_e}{1 + bC_e} \quad (5)$$

$$R_L = \frac{1}{1 + bC_m} \quad (6)$$

where Q_0 is the maximum adsorption capacity per unit mass of adsorbent (mg/g) and b is Langmuir constant related to binding energy of the adsorption system (L/mg) which shows the affinity between adsorbent and adsorbate. By determining R_L value, a dimensionless separation factor or equilibrium parameter, the adsorption is deemed "favorable" or "unfavorable". If the isotherm is unfavorable, $R_L > 1$, linear if $R_L = 1$, favorable for $0 < R_L < 1$ and irreversible is $R_L = 0$. In this study, for CNF in 20, 40 and 60°C, the R_L is between 0 and 1 indicating that the isotherm is favorable.

Freundlich isotherm is expressed as

$$q_e = K_F C_e^{1/n} \quad (7)$$

where K_F and $1/n$ are the Freundlich constants, where K_F represents the relative adsorption capacity of the adsorbent and n, the degree of dependence of adsorption on the equilibrium dye concentration.

Table 2 Data for Langmuir and Freundlich models

Temp. (°C)	Langmuir Model [a]				Freundlich Model [b]		
	Q_0	b	R_L	R^2	K_F	n	R^2
20	122.2	0.178	0.022	0.996	12.8	4.46	0.859
40	114.6	0.261	0.015	0.998	13.7	4.52	0.806
60	110.6	0.253	0.016	0.995	37.5	4.24	0.745

[a] Q_0 (mg/g) = maximum adsorption capacity; b (L/mg) = constant related to adsorption the adsorption energy; R_L = equilibrium parameter;
[b] K_F ((mg/g)(L/mg)$^{1/n}$) = relative adsorption capacity; n = degree of dependence of adsorption

All Langmuir isotherms appeared to fit well for all temperatures, all R^2 values were more than 0.99 which confirmed that the experimental data can be explained by Langmuir isotherm. Maximum adsorption, Q_0 decreases at higher temperature indicating a better adsorption at lower temperature, however, b value increases at higher temperature. Q_0, b, R_L and R^2 values are compiled in Table 2. Whereas, for Freundlich isotherms, the K_F and n values decrease at higher temperature, indicating again a better adsorption at lower temperature. However, the Freundlich isotherm does not appear to fit well for CNF implying that it is a non-heterogeneous adsorption. This indicates that the adsorption is monolayer as opposed to Freundlich isotherm which is not restricted to monolayer. Maximum adsorption for MB is determined to be 122.2 mg/g, in comparison, the maximum adsorption for CNC reported are 101 mg/g [6] and 118 mg/g [5] respectively, while for TEMPO mediated oxidized CNF aerogel is 3.7 mg/g [7]. In this study, we have found that the yield of CNF extracted from KC is 55%, whereas extraction of CNC from the same source yielded only 15.7% [37]. A considerable amount of potential adsorbent is lost due to processing alone if CNC were to be used as an adsorbent.

Cellulose, containing only hydroxyl group on its surface is hardly a good adsorbent for cationic adsorbates. Cationic dyes have a very weak affinity towards cellulose [45] as demonstrated by model compound of cellulose such as microcrystalline cellulose, with Q_0 of only 0.11 mg/g on MB [46]. Cellulosic material, such as CNC, is extracted using sulfuric acid. CNC is esterified while negatively charged sulfate is introduced on its surface [5, 47]. The charged sulfate group on CNC's surface is responsible for the adsorption of MB [5]. This differs from CNF produced in this study, in which the available adsorption sites are already available in hemicelluloses. Furthermore, CNF has a high surface area which can be chemically modified and tailored to enhance its adsorption performance.

Effect of Acid Hydrolysis on Adsorption

Table 3 Effect of hydrolysis on adsorption performance

Sample	Langmuir Model [a]			
	Q_0	b	R_L	R^2
CNF	122.2	0.178	0.022	0.996
AH10	89.17	0.499	0.079	0.939
AH30	85.72	0.393	0.010	0.979
AH90	72.45	0.214	0.018	0.930

[a] Q_0 (mg/g) = maximum adsorption capacity; b (L/mg) = constant related to adsorption the adsorption energy; R_L = equilibrium parameter

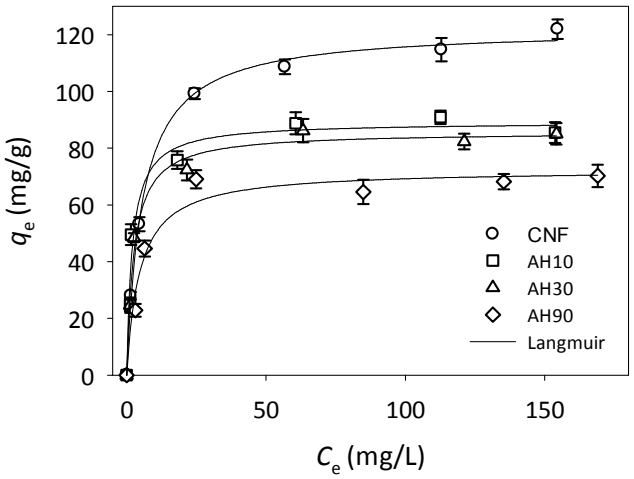

Fig. 8 Effect of acid treatment on the adsorption performance of CNF.

Langmuir isotherm was fitted for all samples of different acidic treatment times. Q_o decreases with increasing acid treatment time as shown in Table 3. All isotherms were deemed favorable. The reduction in adsorption performance may be due to the reduction in hemicellulose and lignin contents where most of the functional groups responsible for adsorption are located. A small amount of carboxylic functional groups introduced during pulping process are usually pointed out as adsorption sites for MB [48].

Cationic dye and cations show a greater affinity towards hemicellulose and lignin [45, 49, 50]. After delignification process, hemicellulose and a small amount of lignin remained in holocellulose as evidenced by the compositional analysis. In compositional analysis, the lignin content determined are lignins bonded to xylan chain [28, 51-53]. Acid-soluble lignin (ASL) is formed during dilute hydrolysis process [54], while the insoluble part of lignin, after concentrated and dilute hydrolysis, forms acid-insoluble lignin (AIL). As a result, acidic hydrolysis treatment will reduce the xylan chain length and lignin content, in which fragmented hemicellulose-lignin will be produced due to random scission of backbone xylan.

Hemicellulose of kenaf is composed of backbone xylan with side chains of O-acetyls and 4-O-methylglucuronic acids [29, 55]. Acidic hydrolysis treatment decreases the available O-acetyls and 4-O-methylglucuronic acids due to random chain scission of ether linkages in hemicellulose. The decrement of acetyl content in samples of increasing hydrolysis treatment time indicates that O-acetylated xylopyranose in hemicellulose is lost due to acidic hydrolysis (refer Table 1). Acetylated natural fibers have been shown to significantly increase the adsorption capacity of cationic dyes [56]. Therefore, it is crucial to retain as much acetyl groups as possible. In addition, 4-O-methylglucuronic acid which contains carboxyl functional group is an ion-exchange site for MB [56], may also have been reduced due to the treatment.

Owing to a low degree of polymerization in hemicellulose, extracted hemicellulose is water soluble, therefore, hemicellulose based adsorbent are usually supported in composites. Hemicellulose composites such as hemicellulose-latex reported a modest Q_0 value of 95.42 mg/g [57]. In another example, cellulose extracted from poplar wood which is delignified and its hemicellulose removed is used to produce CNF aerogel [7]. Without hemicellulose, CNF aerogel has a low adsorption capacity of 3.70 mg/g and 4.15 mg/g towards MB and toluidine blue (TB) respectively [7].

Despite the low amount of residual lignin in CNF after delignification, it may be beneficial for MB adsorption. During delignification, acidified-chlorite generates chlorine dioxide which is the active species used to degrade lignin. The degradation mechanism by chlorine dioxide is complex and generally known to form end-products of quinones [58] and muconic acids [59]. These degraded lignin compounds contain functional groups of carboxyl, methoxyl, aliphatic and phenolic hydroxyls, etc. [60]. It is unclear what is the role of residual lignin in CNF on the adsorption of cationic dyes. However, lignin-formaldehyde and alkali extracted lignin have been shown to adsorb MB with Q_0 values of 34.20 mg/g [61] and 121.20 mg/g [62] respectively.

In conclusion, the reduction in adsorption performance can be attributed to the reduction in hemicellulose content (acetyl) and the reduction of available adsorption sites (lignin).

Desorption and Regeneration

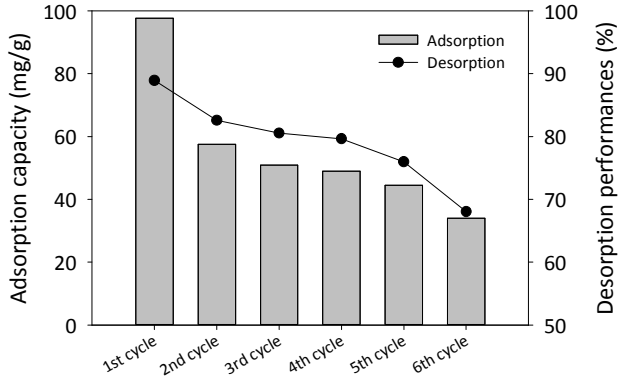

Fig. 9 Regeneration performance of CNF

Desorption of MB is possible by protonating CNF using HCl. Protonation opens up previously active sites for the next cycle of adsorption by desorbing MB adsorbed on CNF. After six cycles of adsorption-desorption processes, > 70 % of dye can be desorbed. However, the adsorption performance after six cycles dropped to 34 %.

The decrement in performance could be due to pre-adsorb MB and aggregation of CNF during desorption. In this study, CNF is stabilized by Na^+ counter-ions. The addition of HCl during desorption process disrupts the repulsion between CNF. This may cause CNF to aggregate which in turn reduces the

total surface area available for consecutive adsorption cycle. Pre-adsorbed MB is also trapped inside these aggregations causing incomplete desorption.

Conclusions

In this study, CNF with various hemicellulose content are produced using acid-chlorite bleaching (delignification) followed by high speed blender disintegration method. Hemicellulose facilitates defibrillation of holocellulose as non-acid treated KC holocellulose produces a more homogeneous CNF compared to acid treated holocellulose. This study also demonstrates that the CNF could be a potential adsorbent due to its rapid adsorption behavior, in which equilibrium is achieved after 1 min. The effects of several adsorption parameters, such as pH, adsorbent dosage, temperature and dye concentration, on the dye uptake, were investigated. Hemicellulose also helps in adsorption as reducing hemicellulose in CNF rendering it less likely to adsorb dye. Up-scaling CNF production to an industrial level may make this process more cost efficient.

Acknowledgements

The authors would like to thank Centre of Research and Instrumentation (CRIM), UKM for their assistance in TEM imaging and ATR-FTIR analysis. This research was supported by DIP-2014-013, LRGS/TD/2012/USM-UKM/PT/04 and ERGS/1/2012/STG05/UKM/01/4.

Notes and references

School of Applied Physics, Faculty of Science and Technology, Universiti Kebangsaan Malaysia, 43600 Bangi, Selangor, Malaysia. Fax: 603 8921 3777; Tel: 603 8921 5473; E-mail: chia@ukm.edu.my / chiachinhua@yahoo.com

Electronic Supplementary Information (ESI) available: [details of any supplementary information available should be included here]. See DOI: 10.1039/b000000x/

1. M. A. Barakat, *Arabian J. Chem.*, 2011, **4**, 361-377.
2. M. Peng, L. M. Vane and S. X. Liu, *J. Hazard. Mater*., 2003, **98**, 69-90.
3. A. Mittal, J. Mittal, A. Malviya, D. Kaur and V. K. Gupta, *J. Colloid Interface Sci.*, 2010, **343**, 463-473.
4. K. Hunger, ed., *Industrial dyes:chemistry, properties, applications*, Wiley, Weinheim, 2003.
5. R. Batmaz, N. Mohammed, M. Zaman, G. Minhas, R. Berry and K. Tam, *Cellulose*, 2014, **21**, 1655-1665.
6. X. He, K. B. Male, P. N. Nesterenko, D. Brabazon, B. Paull and J. H. T. Luong, *ACS Appl. Mater. Interfaces*, 2013, **5**, 8796-8804.
7. W. Chen, Q. Li, Y. Wang, X. Yi, J. Zeng, H. Yu, Y. Liu and J. Li, *ChemSusChem*, 2014, **7**, 154-161.
8. G. Siqueira, J. Bras and A. Dufresne, *Polymers*, 2010, **2**, 728-765.
9. D. Klemm, F. Kramer, S. Moritz, T. Lindström, M. Ankerfors, D. Gray and A. Dorris, *Angew. Chem.*, 2011, **50**, 5438-5466.
10. A. F. Turbak, F.W. Synder, 1984, *Nonwovens Symposium*, 115-124.
11. S. Iwamoto, A. N. Nakagaito, H. Yano and M. Nogi, *Appl. Phys. A*, 2005, **81**, 1109-1112.
12. A. Isogai, T. Saito and H. Fukuzumi, *Nanoscale*, 2011, **3**, 71-85.
13. M. Pääkkö, M. Ankerfors, H. Kosonen, A. Nykänen, S. Ahola, M. Österberg, J. Ruokolainen, J. Laine, P. T. Larsson, O. Ikkala and T. Lindström, *Biomacromolecules*, 2007, **8**, 1934-1941.
14. Q. Q. Wang, J. Y. Zhu, R. Gleisner, T. A. Kuster, U. Baxa and S. E. McNeil, *Cellulose*, 2012, **19**, 1631-1643.
15. B. Deepa, E. Abraham, B. M. Cherian, A. Bismarck, J. J. Blaker, L. A. Pothan, A. L. Leao, S. F. de Souza and M. Kottaisamy, *Bioresour. Technol*., 2011, **102**, 1988-1997.
16. K. Spence, R. Venditti, O. Rojas, Y. Habibi and J. Pawlak, *Cellulose*, 2011, **18**, 1097-1111.
17. N. Lavoine, I. Desloges, A. Dufresne and J. Bras, *Carbohydr. Polym.*, 2012, **90**, 735-764.
18. T. Saito, Y. Nishiyama, J.-L. Putaux, M. Vignon and A. Isogai, *Biomacromolecules*, 2006, **7**, 1687-1691.
19. M. Henriksson, G. Henriksson, L. A. Berglund and T. Lindström, *Eur. Polym. J.*, 2007, **43**, 3434-3441.
20. S. Iwamoto, K. Abe and H. Yano, *Biomacromolecules*, 2008, **9**, 1022-1026.
21. L. E. Wise, M. Murphy and A. A. D'Addieco, *Pap. Trade J.*, 1946, **122**, 35 - 43.
22. R. Kumar, F. Hu, C. A. Hubbell, A. J. Ragauskas and C. E. Wyman, *Bioresour. Technol.*, 2013, **130**, 372-381.
23. Q. Cheng, S. Wang and T. G. Rials, *Composites, Part A*, 2009, **40**, 218-224.
24. L. Suryanegara, A. N. Nakagaito and H. Yano, *Compos. Sci. Technol.*, 2009, **69**, 1187-1192.
25. K. Dimic-Misic, P. A. C. Gane and J. Paltakari, *Ind. Eng. Chem. Res.*, 2013, **52**, 16066-16083.
26. G. Zheng, Y. Cui, E. Karabulut, L. Wågberg, H. Zhu and L. Hu, *MRS Bull.*, 2013, **38**, 320-325.
27. N. Ninan, M. Muthiah, I.-K. Park, A. Elain, S. Thomas and Y. Grohens, *Carbohydr. Polym.*, 2013, **98**, 877-885.
28. A. Sluiter , B. Hames , R. Ruiz , C. Scarlata , J. Sluiter , D. Templeton and D. Crocker*; NREL/TP-510-42618*, 2010.
29. M. K. Nacos, P. Katapodis, C. Pappas, D. Daferera, P. A. Tarantilis, P. Christakopoulos and M. Polissiou, *Carbohydr. Polym.*, 2006, **66**, 126-134.
30. K. Lundquist, R. Simonson and K. Tingsvik, *Sven. Papperstidn.*, 1983, **86**, 44-47.
31. M. B. Foston, C. A. Hubbell and A. J. Ragauskas, *Materials*, 2011, **4**, 1985-2002.
32. K. Wickholm, E.-L. Hult, P. Larsson, T. Iversen and H. Lennholm, *Cellulose*, 2001, **8**, 139-148.
33. K. Uetani and H. Yano, *Biomacromolecules*, 2010, **12**, 348-353.
34. R. Zuluaga, J. L. Putaux, J. Cruz, J. Vélez, I. Mondragon and P. Gañán, *Carbohydr. Polym.*, 2009, **76**, 51-59.
35. F. Jiang, S. Han and Y.-L. Hsieh, *RSC Adv.*, 2013, **3**, 12366-12375.
36. C. Y. Liang and R. H. Marchessault, *J.Polym. Sci.*, 1959, **37**, 385-395.
37. H. C. Chan, C. H. Chia, S. Zakaria, I. Ahmad and A. Dufresne, *BioResources,* 2012, **8**, 785-794.
38. C. R. Orton, D. Y. Parkinson, P. D. Evans and N. L. Owen, *Appl. Spectrosc.*, 2004, **58**, 1265-1271.

39. G. Chinga-Carrasco, *Nanoscale Res. Lett.*, 2011, **6**, 417.
40. M. Paakko, J. Vapaavuori, R. Silvennoinen, H. Kosonen, M. Ankerfors, T. Lindstrom, L. A. Berglund and O. Ikkala, *Soft Matter*, 2008, **4**, 2492-2499.
41. M. S. Sajab, C. H. Chia, S. Zakaria, S. M. Jani, M. K. Ayob, K. L. Chee, P. S. Khiew and W. S. Chiu, *Bioresour. Technol.*, 2011, **102**, 7237-7243.
42. M. Doğan, H. Abak and M. Alkan, *J. Hazard. Mater.*, 2009, **164**, 172-181.
43. P. Janoš, S. Coskun, V. Pilařová and J. Rejnek, *Bioresour. Technol.*, 2009, **100**, 1450-1453.
44. Y. C. Wong, Y. S. Szeto, W. H. Cheung and G. McKay, *Process Biochem.*, 2004, **39**, 695-704.
45. T. Drnovšek and A. Perdih, *Dyes Pigm.*, 2005, **67**, 197-206.
46. R. Bouhdadi, S. Benhadi, S. Molina, B. George, M. El Moussaouiti and A. Merlin, *Maderas: Cienc. Tecnol.*, 2011, **13**, 105-116.
47. X. Dong, J.-F. Revol and D. Gray, *Cellulose*, 1998, **5**, 19-32.
48. C. Kaewprasit, E. Hequet, N. Abidi and J. P. Gourlot, *J. Cotton Sci.*, 1998, **2**, 164-173.
49. F. Perdih and A. Perdih, *Cellulose*, 2011, **18**, 1139-1150.
50. R. B. Garcia-Reyes and J. R. Rangel-Mendez, *J. Chem. Technol. Biotechnol.*, 2009, **84**, 1533-1538.
51. G. Moxley and Y. H. P. Zhang, *Energy Fuels*, 2007, **21**, 3684-3688.
52. TAPPI, T 249 cm-00, 2000.
53. S. Yasuda, K. Fukushima and A. Kakehi, *J. Wood Sci.*, 2001, **47**, 69-72.
54. Y. Matsushita, A. Kakehi, S. Miyawaki and S. Yasuda, *J. Wood Sci.*, 2004, **50**, 136-141.
55. A. Ebringerová, Z. Hromádková and T. Heinze, in *Polysaccharides I*, ed. T. Heinze, Springer Berlin Heidelberg, 2005, vol. 186, pp. 1-67.
56. R. Gong, Y. Sun, J. Chen, H. Liu and C. Yang, *Dyes Pigm.*, 2005, **67**, 175-181.
57. X.-F. Sun, Q. Ye, Z. Jing and Y. Li, *Polym. Compos.*, 2014, **35**, 45-52.
58. B. N. Brogdon, D. G. Mancosky and L. A. Lucia, *J. Wood Chem. Technol.*, 2005, **24**, 201-219.
59. H. Sixta, ed., *Handbook of Pulp*, Wiley-VCH Verlag GmbH, 2008, pp. 708-798.
60. J. Liu and X. F. Zhou, *Sci. Iran.*, 2011, **18**, 486-490.
61. N. Consolin Filho, E. C. Venancio, M. F. Barriquello, A. A. W. Hechenleitner and E. A. G. Pineda, *Eclética Quím.*, 2007, **32**, 63-70.
62. Q. Feng, H. Cheng, J. Li, P. Wang and Y. Xie, *BioResources*, 2014, **9**, 3602-3612.

Table of Contents

Graphics Abstract:

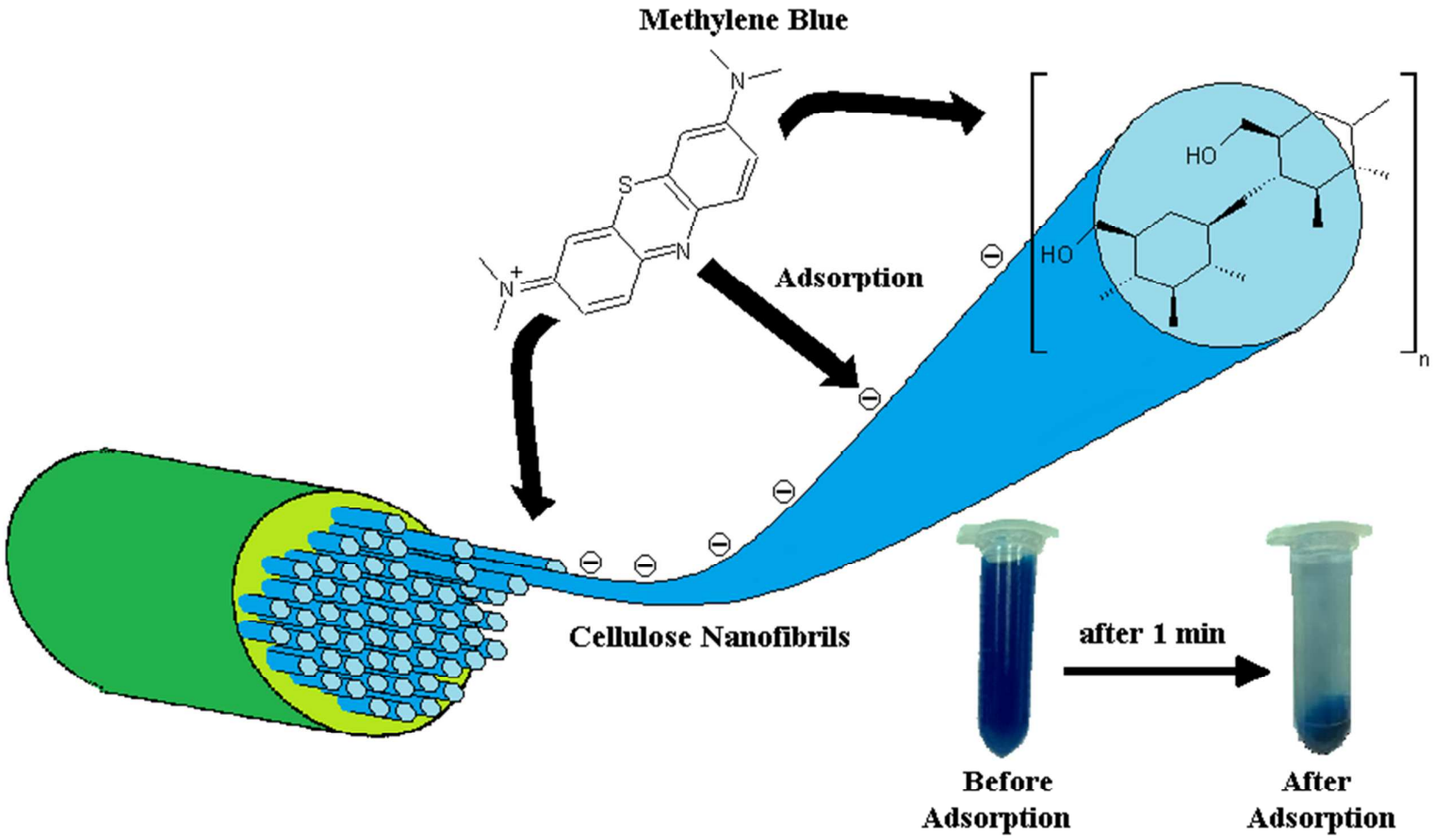

Highlights

- The effect of acid treatment towards the degree of defibrillation.
- Rapid uptake of cationic dye
- Hemicellulose responsible for dye uptake